Energy transfer and 1.54 μm emission in amorphous silicon nitride films

S. Yerci,[1] R. Li,[1] S. O. Kucheyev,[2] T. van Buuren,[2] S. N. Basu,[3,4] and L. Dal Negro[1,3,a)]
[1]*Department of Electrical and Computer Engineering, Boston University, 8 Saint Mary's Street, Boston, Massachusetts 02215–2421, USA*
[2]*Lawrence Livermore National Laboratory, Livermore, California 94551, USA*
[3]*Division of Materials Science and Engineering, Boston University, 15 Saint Mary's Street, Brookline, Massachusetts 02446, USA*
[4]*Department of Mechanical Engineering, Boston University, 110 Cummington Street, Boston, Massachusetts 02215, USA*

(Received 14 May 2009; accepted 1 July 2009; published online 22 July 2009)

Er-doped amorphous silicon nitride films with various Si concentrations ($Er:SiN_x$) were fabricated by reactive magnetron cosputtering followed by thermal annealing. The effects of Si concentrations and annealing temperatures were investigated in relation to Er emission and excitation processes. Efficient excitation of Er ions was demonstrated within a broad energy spectrum and attributed to disorder-induced localized transitions in amorphous $Er:SiN_x$. A systematic optimization of the 1.54 μm emission was performed and a fundamental trade-off was discovered between Er excitation and emission efficiency due to excess Si incorporation. These results provide an alternative approach for the engineering of sensitized Si-based light sources and lasers. © *2009 American Institute of Physics*. [DOI: 10.1063/1.3184790]

Rare-earth doping of silicon-based structures provides a valuable approach for 1.54 μm light-emitting devices, which could be monolithically integrated atop the widespread silicon electronics platform, enabling inexpensive integration of on-chip optical components. Rare-earth doping of Si nanostructures is motivated by the recent discovery of efficient energy transfer between Si nanocrystals embedded in SiO_2 and erbium (Er) ions.[1–5] More recently, almost 60% efficient and nanosecond-fast energy transfer to Er ions have been demonstrated in silicon nitride matrices containing a high density of small (2 nm) Si nanocrystals induced by thermal annealing steps.[6–10] The high refractive index (2.1–2.5) and the favorable electrical transport properties of silicon-rich silicon nitride have led to the recent demonstration of Er-doped photonic crystal nanocavities[11] and electrically pumped superlattice structures.[12] However, little is known about the nature and the optimization conditions of Er emission and sensitization in amorphous silicon nitride. This materials platform could potentially result in the fabrication of active devices with faster modulation speeds, larger optical mode confinement, and reduced free carrier losses at 1.54 μm compared to Si-rich oxide-based photonic structures.[6–13]

In this paper, we study the Er emission and excitation processes in Er-doped amorphous silicon nitride films with different Si concentrations (SiN_x $x \leq 1.33$) in the range 43–50 at. % (refractive indices are in the range of 2.05–2.37), which is close to the equilibrium stoichiometry (43 at. %). We used Rutherford backscattering spectrometry (RBS) and high-resolution transmission electron microscopy (HRTEM) to quantify the amount of Si, N, and Er concentrations in the films, and to investigate the microstructure of the films, respectively. Continuous wavelength (CW), time-resolved photoluminescence (PL), and PL excitation spectroscopy (PLE) were performed in order to understand the role of excess Si and annealing temperature in the optimization of Er excitation and 1.54 μm emission in $Er:SiN_x$ fabricated by reactive cosputtering.

$Er:SiN_x$ films with Si concentrations between 43 and 50 at. % and thicknesses of approximately 350 nm were fabricated by N_2 reactive magnetron cosputtering using Si and Er targets in a Denton Discovery 18 confocal-target sputtering system. The relative concentrations of Si and N atoms in the samples were controlled by varying the N_2/Ar gas flow ratio. Si and Er cathode powers and deposition pressure were kept constant for all samples. Post annealing processes were performed in a rapid thermal annealing furnace at temperatures between 600 and 1150 °C for 200 s under forming gas (5% H_2, 95% N_2) atmosphere to obtain the optimum Er PL intensity (I_{PL}) and lifetime (τ_{PL}) for samples with different Si concentrations. The transmission spectra of the samples were measured between 200 and 1800 nm. The refractive indices of the samples were obtained by spectroscopic ellipsometry (A. J. Woollam VASE) using the Cauchy–Urbach dispersion model. Depth profiles of Si, N, and Er atoms were studied by RBS with 2 MeV ^4He ions incident along the direction normal to the sample surface and backscattered to 164°. Analysis of RBS spectra was done with stopping powers and scattering cross sections from the RUMP code[14] with an assumption of a constant atomic density (9.53×10^{22} atoms/cm^3) and a layer composition of SiN_xEr_y. HRTEM studies of the samples in cross section were carried out using a JEOL 2010 operated at 200 kV, with a point-to-point resolution of 0.19 nm. Selected area electron diffraction (SAED) studies of the films in cross section were carried out to identify if Si nanocrystals were present in the films. CW room temperature Er I_{PL} and τ_{PL} were excited nonresonantly using a 458 nm line of an Ar ion laser (Spectra Physics, 177–602) modulated by a mechanical chopper and detected using either an InGaAs (Oriel 70368) or an extended photomultiplier tube (Hamamatsu R5509–73) detector coupled to an oscilloscope. A monochromatized Xe lamp was used as light source in PLE experiments.

a)Author to whom correspondence should be addressed. Electronic mail: dalnegro@bu.edu.

 © 2009 American Institute of Physics

Downloaded 23 Sep 2009 to 128.197.27.9. Redistribution subject to AIP license or copyright; see http://apl.aip.org/apl/copyright.jsp

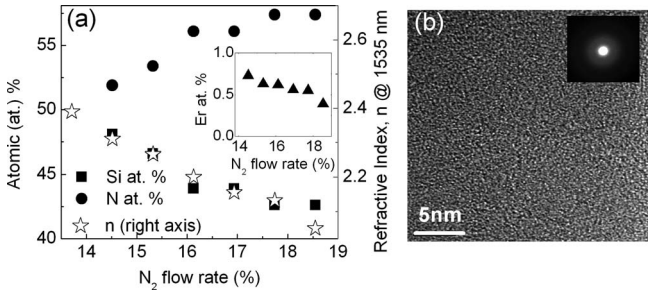

FIG. 1. (a) Relative atomic (at. %) concentrations of Si (squares), N (circles), and Er (triangles in the inset), and refractive indices of the films measured by ellipsometer at 1550 nm (open stars) as a function of N_2 flow rate percent. (b) HRTEM micrograph of a sample with a relative Si concentration of 48 at. % annealed at 900 °C for 200 s under forming gas (N_2/H_2) environment. The SAED pattern of the sample is shown in the inset.

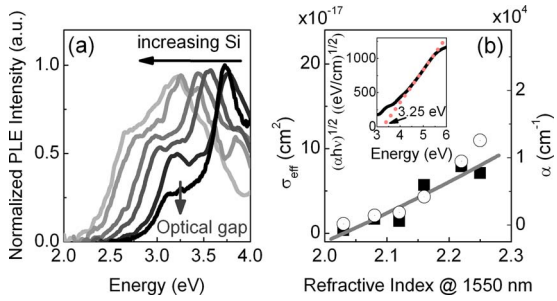

FIG. 2. (Color online) (a) Normalized PLE spectra collected at 1.54 microns from Er:SiN_x samples with various excess Si at. %. (b) The effective excitation cross sections σ_{eff} (squares) and the absorption coefficients α at 458 nm (circles) of the Er:SiN_x samples with different excess Si at. %. The straight line is to guide the eye. In the inset: The optical gap calculated from the Tauc plot of the stoichiometric sample which is highlighted with an arrow in (a).

Figure 1(a) shows the relative atomic concentrations of Si and Er atoms and the refractive indices of the films as a function of the percentage of nitrogen gas flow rate (N_2 flow rate percent) to the total gas rate. We have found that by decreasing the N_2 flow rate percent, the nitrogen atomic concentration in the films decreases while both the Si and Er [Fig. 1(a), inset] concentrations increase. This is readily understood since more Ar ions are available to sputter Si and Er atoms at small N_2 flow rate percent, limiting Si reactions and resulting in Si-rich (substoichiometric) films. The RBS analysis resulted in homogenously distributed Er ions throughout the films with concentrations varying between 3.7×10^{20} and 4.7×10^{20} Er/cm^3 for all the samples. As shown in Fig. 1(a), the measured refractive indices of the films at 1.54 μm correlate directly with their atomic Si concentrations, and increase by reducing the N_2 in the plasma. The Er concentration also increases in the same range but its variation is much less sensitive to the N_2 flow rate percent, as shown in the inset of Fig. 1(a). The HRTEM micrograph and SAED pattern (in the inset) of a sample with a relative Si concentration of 48 at. % (refractive index of 2.25), annealed at 900 °C for 200 s is shown in Fig. 1(b). HRTEM and SAED analysis demonstrate an amorphous structure with no evidence of Si nanocrystals. This is in stark contrast with the behavior of Si-rich nitride films with comparable refractive indices fabricated by direct magnetron cosputtering, which results in the nucleation of Si nanocrystals when annealed within the same temperature range.[8] It is well known that a considerable range in the compositions and structural properties of dielectric films can be obtained depending on the sputtering method and deposition conditions.[15] However, it is also important to note that our HRTEM analysis cannot exclude the formation of very small (<2 nm) amorphous Si clusters in the films, which is consistent with the existence of a two phase system, amorphous Si and SiN_x, as observed by x-ray emission studies on the same samples.[16]

The normalized PLE spectra collected at the 1.54 μm Er emission are shown in Fig. 2(a) for samples with different Si concentrations and demonstrate that Er ions can be excited nonresonantly within a very broad spectral range.[17] In addition, we show that the PLE spectra shift to longer wavelengths by increasing the Si content in the film. This behavior is related to the similar redshift in the optical bandgap of SiN_x, which we determined from the Tauc plot of the absorption data [Fig. 2(b), inset]. The lineshape of the PLE spectra, shown in Fig. 2(a), is typical of amorphous materials and consists of two separate regimes; an exponential increase at energies corresponding to the band tail absorption in the SiN_x matrix followed by a sudden decrease at higher photon energies.[18,19] The PLE roll off at high photon energies can be attributed to reduced energy transfer efficiency due to a smaller excitation volume and the carrier thermalization into efficient nonradiative trap states.[19] Figure 2(a) shows that energy transfer can occur at energies above and below the optical gap. In particular, these data show that Er ions can be nonresonantly excited even below the optical bandgap of the embedding amorphous matrix where disorder-induced localized states in the SiN_x band tails can play a direct role in the sensitization of Er ions.

We have further quantified the matrix-mediated Er excitation process by measuring the Er excitation cross section σ_{exc} for samples with different Si concentrations. The parameter σ_{exc} can be directly measured in the weak excitation regime by the linear dependence of the Er PL rise time versus the pumping photon flux.[4,5,8] In Fig. 2(b), we show the measured σ_{exc} values at the 458 nm nonresonant Er excitation wavelength as a function of the Si concentration in our films. The Er excitation cross section increases with the Si concentration in the films. Interestingly, the measured values of σ_{exc}, which are in the 10^{-18}–10^{-17} cm^2 range, are comparable with values reported for Er doped silicon nanocrystals embedded in silicon nitride and in silicon oxide matrices.[4,5,8] Figure 2(b) demonstrates that σ_{exc} and the measured absorption coefficient (from ellipsometry) at 458 nm show a similar trend with the Si concentration in the films. This indicates that the increase in σ_{exc} is a direct result of the enhanced absorption coefficient of Si-rich films.

An equally important aspect of engineering Si-based light sources is the optimization of the sensitized Er emission. In this paper, we systematically investigate the 1.54 μm Er emission and decay time for a set of 49 samples with seven different Si concentrations between 43 and 50 at. % (refractive indices between 2.05 and 2.37) and annealed a temperature range of 600–1150 °C. All the samples have been excited at 458 nm under identical pumping conditions and the results are shown in the Fig. 3. The integrated Er PL intensities of samples with high Si concentrations are optimized at lower annealing temperatures as shown in Fig. 3(a) and previously reported Si-rich silicon nitride films by cosputtering.[8] However, we see that similar PL intensities can be achieved across a large range of Si concentrations by

Downloaded 23 Sep 2009 to 128.197.27.9. Redistribution subject to AIP license or copyright; see http://apl.aip.org/apl/copyright.jsp

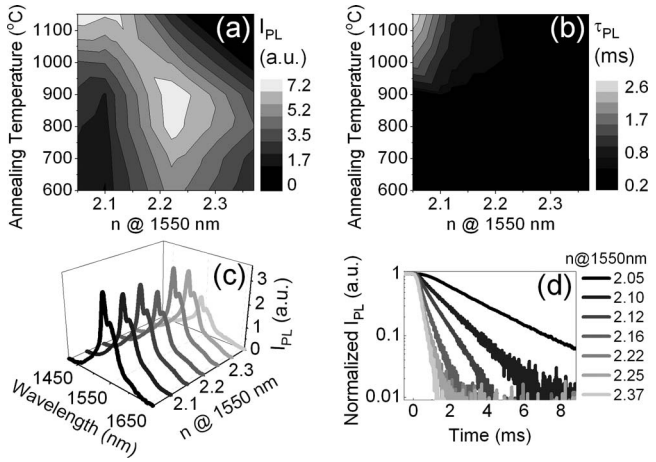

FIG. 3. (a) Er integrated PL intensity (I_{PL}) of SiN_x samples with Si at. % between 43 and 50 (refractive indices between 2.05 and 2.37) annealed at temperatures between 600 and 1150 °C, with (b) corresponding Er PL lifetimes (τ_{PL}) vs refractive indices of the films. (c) Er PL spectra corresponding to samples with refractive indices n=2.05, 2.10, 2.12, 2.16, 2.12, 2.25, and 2.37, and annealed at the optimum temperatures shown in panel (a). (d) PL decay traces of the samples in panel (c).

annealing the samples at different temperatures [Fig. 3(c)]. In particular, the optimization of Er emission occurs along the diagonal white region of Fig. 3(a), implying that the optimum 1.54 μm emission from samples with low Si concentrations requires the highest annealing temperatures. This effect is particularly visible in Fig. 3(c), which shows the Er emission spectra of several samples with different Si concentrations and annealed at the different optimal temperatures. The results show that the Er emission efficiency, which is proportional to the Er emission lifetime, is optimized for samples with the lowest Si concentration annealed at the highest temperatures as shown in Fig. 3(b).[20] In fact, the Er emission lifetime decreases dramatically by increasing the Si concentration in the films. Samples of almost equilibrium stoichiometry (very low excess Si) annealed at the highest temperatures (1150 °C) show the longest Er lifetime of ~2.6 ms. The behavior of the Er emission decay traces with increasing Si concentrations are displayed in Fig. 3(d). PL decay traces of the 1.54 μm can be fitted with a single exponent for all samples indicating the absence of detrimental processes such as upconversion.

The data in Figs. 2 and 3 demonstrate the existence of a fundamental trade-off between the Er excitation efficiency due to energy transfer and the Er emission efficiency. An optimal annealing temperature exists for the Er emission in SiN_x samples with different stoichiometries, pointing toward a complex interplay between the passivation of nonradiative defects in the matrix and the creation of extrinsic defect states associated to the incorporation of excess Si atoms in the SiN_x matrix.[21] Although a microscopic picture is still lacking, our data demonstrate that disorder-induced localized states in SiN_x can directly be involved in the energy transfer process to Er ions and result in 1.54 μm emission sensitization even below the SiN_x optical absorption gap in the absence of Si nanocrystals.

In conclusion, Er doped amorphous silicon nitride films with different Si concentrations were fabricated by reactive cosputtering. Their 1.54 μm emission and energy transfer properties were investigated using PL and PLE spectroscopy. Our results demonstrated nonresonant, broadband Er excitation without the formation of Si nanocrystals along with the existence of a trade-off between energy transfer and Er emission efficiency. Finally, we presented the optimization of Er PL efficiency from $Er:SiN_x$ by varying Si concentration and annealing temperature. $Er:SiN_x$ films can play an important role in the engineering of sensitized Er emission for the demonstration of Si-based light sources and lasers for on-chip photonic applications.

This work was partially supported by the U.S. Air Force MURI program on "Electrically Pumped Silicon-Based Lasers for Chip-Scale Nanophotonic Systems" supervised by Dr. Gernot Pomrenke. Work at LLNL was performed under the auspices of the U.S. DOE by LLNL under Contract No. DE-AC52-07NA27344.

[1] M. Fujii, M. Yoshida, Y. Kanzawa, S. Hayashi, and K. Yamamoto, Appl. Phys. Lett. **71**, 1198 (1997).
[2] M. Wojdak, M. Klik, M. Forcales, O. B. Gusev, T. Gregorkiewicz, D. Pacifici, G. Franzo, F. Priolo, and F. Iocona, Phys. Rev. B **69**, 233315 (2004).
[3] J. H. Shin, W. Lee, and H. Han, Appl. Phys. Lett. **74**, 1573 (1999).
[4] F. Priolo, G. Franzo, D. Pacifici, V. Vinciguerra, F. Iocona, and A. Irrera, J. Appl. Phys. **89**, 264 (2001).
[5] D. Pacifici, G. Franzo, F. Priolo, F. Iacona, and L. Dal Negro, Phys. Rev. B **67**, 245301 (2003).
[6] N. M. Park, C. J. Choi, T. Y. Seong, and S. J. Park, Phys. Rev. Lett. **86**, 1355 (2001).
[7] L. Dal Negro, J. H. Yi, J. Michel, L. C. Kimerling, S. Hamel, A. Williamson, and G. Galli IEEE J. Sel. Top. Quantum Electron. **12**, 1628 (2006).
[8] L. Dal Negro, R. Li, J. Warga, and S. N. Basu, Appl. Phys. Lett. **92**, 181105 (2008).
[9] R. Li, J. R. Schneck, J. Warga, L. Ziegler, and L. Dal Negro, Appl. Phys. Lett. **93**, 091119 (2008).
[10] L. Dal Negro, R. Li, J. Warga, S. Yerci, S. Basu, S. Hamel, and G. Galli, in *Silicon Nanophotonics: Basic Principles, Present Status and Perspectives*, edited by L. Khriachtchev (World Scientific, Singapore, 2008).
[11] M. Makarova, V. Sih, J. Warga, R. Li, L. Dal Negro, and J. Vuckovic, Appl. Phys. Lett. **92**, 161107 (2008).
[12] J. Warga, R. Li, S. N. Basu, and L. Dal Negro, Appl. Phys. Lett. **93**, 151116 (2008).
[13] D. Navarro-Urrios, A. Patanti, N. Daldosso, F. Gourbilleau, R. Rizk, G. Pucker, and L. Pavesi, Appl. Phys. Lett. **92**, 051101 (2008).
[14] L. R. Doolittle, Nucl. Instrum. Methods Phys. Res. B **9**, 344 (1985).
[15] M. Ohring, *The Materials Science of Thin Films* (Academic, New York, 1992).
[16] J. R. I. Lee and T. van Buuren, personal communication (May 2009).
[17] O. Savchyn, R. M. Todi, K. R. Coffey, and P. Kik, Appl. Phys. Lett. **93**, 233120 (2008).
[18] H. Kato, N. Kashio, Y. Ohki, K. S. Seol, and T. Noma, J. Appl. Phys. **93**, 239 (2003).
[19] R. A. Street, Adv. Phys. **25**, 397 (1976).
[20] A. Polman, J. Appl. Phys. **82**, 1 (1997).
[21] R. Li, S. Yerci and L. Dal Negro, "Temperature Dependence of the Energy Transfer from Amorphous Silicon Nitride to Er Ions," Appl. Phys. Lett. (to be published).

Downloaded 23 Sep 2009 to 128.197.27.9. Redistribution subject to AIP license or copyright; see http://apl.aip.org/apl/copyright.jsp